Mai *et al. Molecular Cancer* (2025) 24:6
https://doi.org/10.1186/s12943-024-02202-9

Molecular Cancer

RESEARCH Open Access

Intra-tumoral *sphingobacterium multivorum* promotes triple-negative breast cancer progression by suppressing tumor immunosurveillance

Zhikai Mai[1†], Liwu Fu[2*], Jiyan Su[1†], Kenneth K.W. To[3], Chuansheng Yang[4] and Chenglai Xia[1*]

Abstract

Background Intratumor-resident bacteria represent an integral component of the tumor microenvironment (TME). Microbial dysbiosis, which refers to an imbalance in the bacterial composition and bacterial metabolic activities, plays an important role in regulating breast cancer development and progression. However, the impact of specific intratumor-resident bacteria on tumor progression and their underlying mechanisms remain elusive.

Methods 16S rDNA gene sequencing was used to analyze the cancerous and paracancerous tissues from breast cancer patients. The mouse models of bearing 4T1 cell tumors were employed to assess the influence of bacterial colonization on tumor growth. Tissue infiltration of regulatory T (Treg) cells and $CD8^+$ T cells was evaluated through immunohistochemistry and flow cytometric analysis. Comparative metabolite profiling in mice tumors was conducted using targeted metabolomics. Differential genes of tumor cells stimulated by bacteria were analyzed by transcriptomics and validated by qPCR assay.

Results We found that *Sphingobacterium* displayed high abundance in cancerous tissues. Intra-tumoral colonization of *Sphingobacterium multivorum* (*S. multivorum*) promoted tumor progression in 4T1 tumor-bearing mice. Moreover, *S. multivorum* diminished the therapeutic efficacy of αPD-1 mAb, which was associated with the increase of regulatory T cell (Treg) infiltration, and decrese of the $CD8^+$ T cell infiltration. Targeted metabolomics revealed a conspicuous reduction of propionylcarnitine in tumors colonized by *S. multivorum* Furthermore, the combination of metabolite propionylcarnitine and *S. multivorum* shown to suppress tumor growth compared that in *S. multivorum* alone in vivo. Mechanistically, *S. multivorum* promoted the secretion of chemokines CCL20 and CXCL8 from tumor cells. CCL20 secreted into the TME facilitated the recruitment of Treg cells and reduced $CD8^+$ T cell infiltration, thus promoting tumor immune escape.

†Zhikai Mai and Jiyan Su contributed equally to this work.

*Correspondence:
Liwu Fu
Fulw@mail.sysu.edu.cn
Chenglai Xia
xiachenglai@smu.edu.cn

Full list of author information is available at the end of the article

Conclusions This study reveals *S. multivorum* suppresses immune surveillance within the TME, thereby promoting breast cancer progression.

Keywords Breast cance, *Sphingobacterium multivorum*, Immune escape, Treg cell, Propionylcarnitine

Background

Breast cancer (BC) is the most common cancer worldwide. The rising incidence of BC especially among the youth population has become a severe threat to women's health [1]. With the advance of microbial detection techniques and the increased understanding about intratumoral microbes, intratumor-resident bacteria are considered an essential regulator within the tumor microenvironment (TME) [2, 3]. These microorganisms typically coexist in equilibrium with the host, influencing physiological processes [4]. Disruption of this balance is implicated in an array of diseases, affecting tumor progression [5, 6], drug resistance [7], and treatment response [8], which attracted increasing attention in various scientific research communities. Several studies have shown that intratumoral microorganisms or their metabolites can contribute to cancer progression and metastasis by modifying the proportion and function of tumor-infiltrating lymphocytes (TILs) in the TME. For instance, intratumor-resident *F. nucleatum* can accelerate breast cancer progression and metastasis via T cell inhibition within the TME [6]. The commensal microbiota-related metabolite trimethylamine N-oxide was also shown to promote $CD8^+$ T cell-mediated immunity against tumors [9]. However, the influence of other potential microorganisms in the tumor and their mechanisms remain largely elusive.

Regulatory T (Treg) cells are physiologically immunosuppressive subpopulations of T cells that play an essential role in maintaining immune tolerance [10]. Treg cells can be divided into natural regulatory T (nTreg) cells and induced regulatory T (iTreg) cells. Both types of Treg cells express the transcription factor FoxP3 [11]. nTreg cells are produced naturally in the thymus, which are mainly responsible for maintaining normal immune tolerance and controlling inflammatory responses [12]. On the other hand, iTreg cells originate from naïve T cells in the periphery. They are induced by signals from the TME, including tumor-derived antigens, cytokines, and other soluble molecules [13]. iTreg cells within the TME can suppress the anti-tumor effects of $CD8^+$ T cells, natural killer cells, and dendritic cells through multiple mechanisms, thereby promoting tumor progression [14].

We identified *Sphingobacterium multivorum* (*S. multivorum*), which showed a high abundance in the tumor tissues of breast cancer patients. *Sphingobacterium* species are aerobic and Gram-negative bacteria, known as opportunistic human pathogens, implicated in serious infections, including cellulitis, endocarditis, meningitis, and bacteremia [15]. Emerging evidence indicates that *Sphingobacterium* presents across diverse clinical samples from cancer patients. For example, *Sphingobacterium* can be detected in the urine of bladder cancer patients [16], fecal samples from colon adenocarcinoma patients [17], the tumor tissues of triple-negative breast cancer [18], intrahepatic cholangiocarcinoma [19], and pancreatic ductal adenocarcinoma [5]. To this end, the effect of *S. multivorum* on breast cancer growth remains to be elucidated.

In this study, we performed 16S rDNA gene sequencing on tumor and paracancerous tissue of breast cancer patients. *S. multivorum* was identified as one of the most abundant residents in tumor tissues. In 4T1 tumor-bearing mouse model, intra-tumoral injection of *S. multivorum* diminished the therapeutic efficacy of αPD-1 mAb, increased Treg cells, and reduced the $CD8^+$ T cell infiltration. Furthermore, targeted metabolomic analysis of tumor tissues showed a substantial decline in the carnitine metabolite propionylcarnitine in the mice injected with *S. multivorum*. Propionylcarnitine inhibited the proportion of Treg cells in mouse spleen lymphocytes in vitro. Mechanistically, *S. multivorum* promoted the release of chemokine CCL20, which reduced the ratio of $CD8^+$ T cells/Treg cells within the TME. Our findings demonstrated that intratumoral *S. multivorum* could influence the proportion and function of TILs and they played a major role in immune surveillance within the TME.

Methods

Patients and samples

Paracancerous tissues ($n=21$) and tumor tissues ($n=20$) were collected from breast cancer patients with informed consent. Demographic information and clinical characteristics of the breast cancer patients are shown in Table S1. The investigation complied with pertinent ethical standards governing human participant research. The collection and use of patient-derived tumor specimens for research was approved by Ethics Committee of Yuebei People's Hospital (Reference KY-2022-057).

Culture of bacteria and cancer cell lines

S.multivorum was purchased from the BeNa Culture Collection and incubated in LB medium under 30℃ aerobic conditions. Human breast cancer cells (4T1, MDA-MB-231, and BT2) were cultured in DMEM (for MDA-MB-231 cells and BT20 cells) or RPMI 1640 (for

4T1 cells). The cell line cultures were maintained at 37℃ and 5% carbon dioxide.

16S rDNA gene sequencing of human breast samples

Tumors were removed surgically, and specimens from the resected breast cancerous tissue and adjacent tissue were harvested under aseptic conditions and placed the specimen on a separate sterile surface. After accurately getting the required tissue, we put the tissue in the preservation tube. All specimens were stored at −80°C till further use. Sequencing of the cDNA library was conducted by Gene Denovo Biotechnology (Guangzhou, China). DNA was extracted from cancerous tissue (n=21) and adjacent tissue (n=20) of breast cancer patients. The quantity and quality of DNA was assessed using a spectrophotometer and agarose gel electrophoresis. Ribosomal 16S rDNA V3-V4 region was amplified with universal primers: forward F (5'-CCTACGGGNGGCWGCAG-3') and reverse R (5'-GGACTACHVGGGTATCTAAT-3') [20]. The amplified DNA fragments were visualized by agarose gel electrophoresis in 2% gel and subsequently extracted and purified using the AxyPrep DNA Gel Extraction kit. Sequencing libraries were constructed employing SMRTbellTM template preparation kits from SMRTbell following the manufacturer's recommendations.

In order to obtain high-quality clean reads, the raw data were filtered using FASTP to remove reads containing more than 10% unknown bases (N) and to exclude reads with less than 50% of bases having a quality score below 20 [21]. The UPARSE pipeline was then employed to cluster valid tags into operational taxonomic units (OTUs) based on a similarity threshold of ≥97%. The most abundant sequence within each cluster was selected as the representative sequence [22].

Alpha diversity analysis was evaluated by Chao, Simpson, Shannon, and the ACE index. Welcht's t-test or Wilcoxon rank test was used for statistical analysis. Comparisons of the microbial community structures were made using the Bray-Curtis dissimilarity index, and the results were depicted by Principal Coordinate Analysis (PCoA). The distinctions in beta diversity among the microbial assemblages were quantitatively analyzed using Analysis of Similarities (ANOSIM). Differences in microbial abundance were analyzed by the LEfSe software, and samples were compared between two groups by the Wilcoxon rank test and screened for differences using the results derived from the LDA method (Linear Discriminant Analysis) [23]. The bacteria were considered to differ between the two groups when the LDA score was ≥2.

Quantitative real-time PCR

MDA-MB-231 and BT20 cell was co-cultured with *S. multivorum* (multiplicity of infection=100) in DMEM with penicillin and streptomycin withdrawn for 6 h, then washed with PBS for 5 times, and RNA was extracted. For propionylcarnitine treatment experiments, RNA was extracted from MDA-MB-231 and BT20 cells after treatment with different concentrations of propionylcarnitine for 24 h. Total RNA was extracted by Total RNA isolation kit (Foregene China), with procedures adhering to the manufacturer's protocol. Specific primers are listed in the Supplementary Materials. The conditions for the PCR amplification of cDNA were as follows: an initial denaturation at 95 °C for 2 min, followed by a total of 40 cycles consisting of a 5s denaturation step at 95 °C and an annealing step of 30 s at 60 °C. Data were calculated using the $2^{-\Delta\Delta Ct}$ method after normalization with the GAPDH expression level in each sample.

RNA-sequencing and analysis

MDA-MB-231 cell was co-cultured with *S. multivorum* (multiplicity of infection=100) in DMEM with penicillin and streptomycin withdrawn for 6 h. Approximately 10^7 cells were harvested, and total RNA was extracted with TRIzol reagent (Thermo Fisher Scientific). After assessing the integrity and quality of the RNA, further verification was performed by RNAase-free agarose gel electrophoresis. After isolation, mRNA was enriched and then fragmented using fragmentation buffer and subsequently reverse transcribed to cDNA. The resulting cDNA library was sequenced by Gene Denovo Biotechnology (Guangzhou, China).

Targeted metabolomics analysis

Targeted metabolomics analysis was performed by Metabo-Profile (Shanghai, China). The tumor tissues of mice in the model group and *S. multivorum* group were analyzed by ultra-performance liquid chromatography-mass spectrometry (UPLC-MS). Briefly, resected tissue specimens were mixed with zirconium oxide beads, deionized water, and methanol inclusive of internal calibrators to facilitate metabolite solubilization. Following several minutes of homogenization, the homogenate was centrifuged, and the resulting supernatant was transferred into a 96-well plate, which was subsequently sealed and subjected to LC-MS analysis [24].

Based on the results of the OPLS-DA model, reliable metabolic markers were screened by Volcano plot. The value of variable influence on projection (VIP)≥1.0 is regarded as significantly different within the tumor [25]. Differential metabolites among mouse tumor tissues were identified using univariate statistical analysis (Student's t-test or Mann-Whitney U-test). Thresholds in the volcano diagram plots were set at $p<0.05$ and $|\log2FC| \geq 0$. Pathway enrichment analysis of differential metabolites was conducted using the Pathway-associated metabolite sets (SMPDB) library.

In vivo experiments

BALB/c mice were purchased from Charles River (Beijing). Breast cancer 4T1 cells (8×10^4 cells/mouse) were subcutaneously injected into the lower right flank of mice. When the tumor size reached 50-100mm^3, the mice were assorted into two cohorts randomly: (1) control group and (2) experimental group injected with *S. multivorum*. The tumor was injected with normal saline or *S. multivorum* (2×10^7 CFU) twice a week. Tumor sizes and body weight were also measured twice a week.

For PD-1 antibody treatment experiments, 4T1 cells (8×10^4 cells/mouse) were subcutaneously injected into the lower right flank of mice. *S. multivorum* (intratumorally) with or without PD-1 antibody (intra-peritoneally) was administered to the tumor-bearing mice after the tumor volume reached 50-100mm^3. 2×10^7 CFU *S. multivorum* or the same volume of saline was intratumorally injected twice a week. Meanwhile, IgG2α isotype control (BioXcell) or PD-1 antibody (BioXcell) was administered intraperitoneally once a week. Group of mice was administered i.p. with 10 μg of αPD-1 mAb and IgG isotype antibody.

For CD8$^+$ T cell depletion experiments, BALB/c mice were injected with CD8 neutralizing antibody (BioXCell) or isotype Control (BioXCell) once a week. Group of mice was administered i.p. with 10 μg of αCD8 mAb and IgG isotype antibody. 2×10^7 CFU *S. multivorum* or the same volume of saline was intra-tumorally injected twice a week.

For 4T1 tumor-bearing mouse model, 2×10^7 CFU of *S. multivorum* were injected into subcutaneous tumors as described above. 150 mg/kg propionylcarnitine was injected into the tumor twice a week. When the tumor volume reached 1500 mm^3, the treatment was terminated, and the mice were euthanized. The volume of the tumors was determined using the formula:

Volumn (mm^3) = 0.5 × longest diameter (mm) × shortest diameter^2(mm).

Immunohistochemistry

Mouse tumor tissues were preserved using 4% paraformaldehyde fixation, embedded within paraffin, and sectioned to a nominal thickness of 4 micrometers. The paraffin-embedded sections were incubated with primary antibodies (CD8, 1:1000 Servicebio, Foxp3, 1:250, Bioss) at 4℃ overnight, followed by incubation with the second antibody at room temperature with protection from light for 1 h. DAB staining and hematoxylin staining were performed on sections following the corresponding standard protocols. Tissue staining was observed under a microscope. Image J was used to score the number of positive cells in the image.

Fluorescence in situ hybridization

The *S. multivorum* probe (5'- TCTCACCGTCTTCGA GCAAGCTCTCCG-3') conjugated with the Cy3 fluorophore (Future Biotech) was used to identify *S. multivorum* colonization within in the mouse tumors. Adhering to the protocols stipulated by the supplier, the tissue samples were dewaxed and soaked in hydrochloric acid, triton, and lysozyme and then blocked with a blocking buffer at 55℃ for 2 h. Afterwards, the tissue samples were incubated with the diluted probe (in 1:100 Hybridization Buffer), allowed to denature at 88℃ for 3 min, equilibrate at 37℃ for 5 min, and hybridize at 37℃ for 48 h. After washing, the probe was stained with DAPI and photographed using a fluorescence microscope.

ELISA assay

MDA-MB-231 or BT20 cells were co-cultured with *S. multivorum* (multiplicity of infection = 100) in DMEM with penicillin and streptomycin withdrawn for 6 h. The culture medium was subjected to centrifugation at 3000×g for 5 min, and the resultant supernatant was filtered. CCL20 and CXCL8 expression were detected by ELISA kit (Abclonal) following the manufacturer recommended procedures.

Tissue pieces were weighed and then homogenized in PBS, maintaining a ratio of 1g of tissue to 9 mL of PBS. The resulting homogenates were then centrifuged at 5000×g at 4℃. The quantities of IFN-γ, CCL20, and CXCL8 in the supernatant was detected by the corresponding ELISA kit (Elabscience) following the manufacturer's instructions.

Flow cytometry

To analyze the tumor-infiltrating lymphocytes (TILs), mice tumor tissue was digested using the Tumor Dissociation Kit (Cat#130-096-730, Miltenyi Biotec) and dissociated with gentleMACS in accordance with the manufacturer's protocol. The resulting sample was passed through a 70 μm cell filter and washed with PBS. Single tumor cells were then resuspended in 5 mL of a 40% Percoll gradient solution (Cat#P8370, Solarbio), carefully layered onto 5 mL of an 80% Percoll solution, and centrifuged at 325 g for 25 min at room temperature. The TILs were collected from the interface between the 40% and 80% Percoll layers.

For mouse spleen lymphocyte extraction, the BALB/c mice were euthanized, and their spleens were promptly removed. Each spleen was placed on a 200-mesh nylon net in a petri dish and gently ground with a syringe while PBS solution was continuously added during the grinding process. The resulting splenic cell suspension was transferred to a centrifuge tube and centrifuged at 350 g for 5 min, after which the supernatant was discarded. Subsequently, 1 mL of ACK red blood cell lysate was added,

and the mixture was gently agitated and left at room temperature for 2 min to facilitate lysis. The sample was then centrifuged again at 350 g for 5 min, resuspended in RPMI 1640 complete medium, and counted.

Similarly, in blood sample preparation, 4 mL of PBS diluted blood was added to the Ficoll layer. Centrifuge 400 g for 30 to 40 min at 18℃-20℃. The middle white membrane (lymphocyte) was sucked into a new centrifuge tube and incubated with flow antibodies.

Cell samples, mouse tumor tissues, and blood samples were incubated with flow antibodies (CD3 FITC, CD4 PE cy7, or CD25 PE, Elabscience) at 4℃ and protected from light. Cell samples were fixed and permeabilized following the manufacturer's instructions by Foxp3 / Transcription Factor Staining Buffer Set (cat#00-5523-00, eBioscience). Cellular specimens were further incubated at room temperature for 30 min with the FoxP3 V450 antibody. Cell samples were assayed by flow cytometry, and data were statistically analyzed by FlowJo software.

Statistical analysis

GraphPad Prism 8 was used for statistical analyses. The samples were tested for normality. If the data were normally distributed, the independent sample *t*-test was used to compare the measured data between the two groups. A univariate analysis of variance (ANOVA) was performed for comparisons among three or more groups. For data that were not normally distributed, the non-parametric Mann-Whitney test was used for comparison and the Wilcoxon signed-rank test was used for matched data. Data are expressed as mean ± standard deviation (SD). p values < 0.05 were considered statistically significant.

Results

S.multivorum was enriched in cancerous tissues from breast cancer patients

To evaluate the correlation between different tumor-resident bacteria and breast cancer development, we performed 16S rDNA gene sequencing analysis on cancerous tissues ($n=21$) and paracancerous tissues ($n=20$) from each breast cancer patient. α-diversity analysis was carried out to investigate the complexity of species in the microbial community for each sample, using the Chao1, ACE, Shannon and Simpson indices. The Chao1 and ACE value reflect the species richness of the bacterial community. On the other hand, the Shannon and Simpson value are associated with the species diversity of the bacterial community, which are influenced by both species richness and species evenness. There were statistically significant differences in Chao and ACE indices, whereas the Simpson and Shannon indices were not significantly different between the tumor and adjacent tissue groups (Fig. 1A). Principal Coordinate Analysis (PCoA) was used to compare the microbial communities of paracancerous and cancerous tissues (Fig. 1B). Notably, *Sphingobacterium* was found in the paracancerous and cancerous tissues of breast cancer patients in genus level. In this cohort, the relative abundance of *Sphingobacterium* was ranked 11th out of 170 bacterial genera (Fig. 1C). Furthermore, the linear discriminant analysis (LDA) effect size (LEfSe) analysis revealed that *Staphylococcus*, *Lactococcus*, *Sphingobacterium*, and *Edaphobacter* were abundant in tumor tissues whereas *Sediminibacterium*, *Tepidiphilus*, *Ralstonia*, and *Bacteroides* were relatively more abundant in the paracancerous tissues (Fig. 1D, E). Intriguingly, we also confirmed the colonization of *Sphingobacterium* at the genus level (Fig. 1F) and the colonization of *S. multivorum* in the paracancerous and cancerous tissues (Fig. 1G), suggesting that *S. multivorum* may represent a prominent intra-tumor resident bacteria in breast cancer.

Tissue-resident *S. Multivorum* accelerated tumor growth in vivo

Given that *S. multivorum* was one of the most abundant bacteria residing in tumor tissues of breast cancer patients, we hypothesized that *S. multivorum* may promote breast cancer progression. Using the 4T1 tumor-bearing mouse model, we investigated the influence of tissue-resident *S. multivorum* on tumor growth in vivo (Fig. 2A). Compared with the control group, 4T1 tumor-bearing mice receiving twice weekly intratumoral injections of 2×10^7 colony-forming units (CFU) of *S. multivorum* exhibited a significant augmentation in tumor size (Fig. 2B) and tumor weight (Fig. 2C). To confirm the colonization of *S. multivorum* within the TME, we detected *S. multivorum* by fluorescence in situ hybridization assay on paraffin sections of mouse tumors. Positive signals were only observed in the tumor paraffin sections from the *S. multivorum*-injected mice, indicating the presence of the *S. multivorum* in the tumor, but not from the control mice (Fig. 2D). These data suggest that colonization of *S. multivorum* within tumors accelerated breast tumorigenesis.

Tumor-infiltrating lymphocytes (TIL) are an important component of the TME. Changes in TILs during tumor progression could be used as a measure of tumor aggressiveness and response to anticancer therapy. We used immunohistochemical staining to detect FoxP3, a specific marker for Treg cells in paraffin sections of tumor tissue. $FoxP3^+$ cells were significantly increased (Fig. 2E) whereas $CD8^+$ T cells were decreased in tumors of mice colonized by *S. multivorum* (Fig. 2F). Data from multicolor flow cytometric analysis further confirmed these findings. We found a similar increase of $CD25^+$ $FoxP3^+$ Treg cells (Fig. 2G) but a reduced infiltration of $CD8^+$ T cells in 4T1 tumor-bearing mice colonized by *S. multivorum*, compared with the control group (Fig. 2H). In

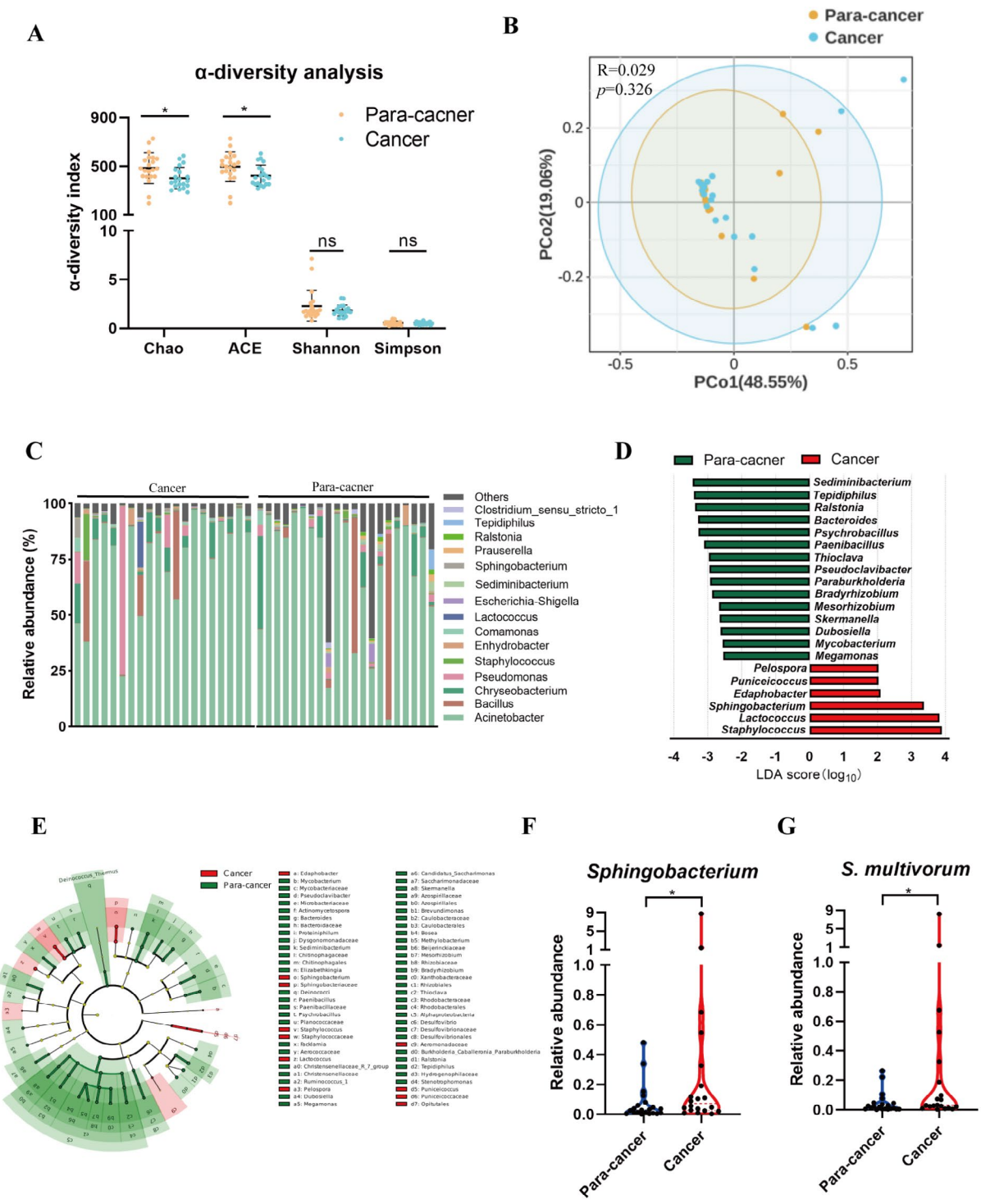

Fig. 1 16S rDNA gene sequencing analysis of tumor and paracancerous tissues of breast cancer patients. (**A**) Chao, ACE, Shannon, and Simpson indices were used to evaluate the relative abundance and homogeneity of microbial communities in cancerous and para-cancerous tissues. (**B**) Differences in microbial communities were compared using principal coordinate analysis (PCoA), and statistical differences were evaluated by analysis of similarities (ANOSIM). (**C**) The bar graph plots each patient's relative abundance of the top 15 enriched genus taxonomies in paracancerous ($n=21$) and cancerous tissues ($n=20$). (**D**, **E**) LEfSe analysis facilitated the calculation of linear discriminant analysis (LDA) scores to quantify the bacterial abundance at the genus level in cancerous and paracancerous tissues from breast cancer patients. The LDA score > 2 was shown. (**F**) The relative abundance of *Sphingobacterium* in breast cancer patients at the genus level using Wilcoxon nonparametric test. (**G**) The relative abundance of *S. multivorum* from breast cancer patients at the species level. Statistical analysis using Wilcoxon nonparametric test. Significance levels are denoted as $*p<0.05$; $**p<0.01$

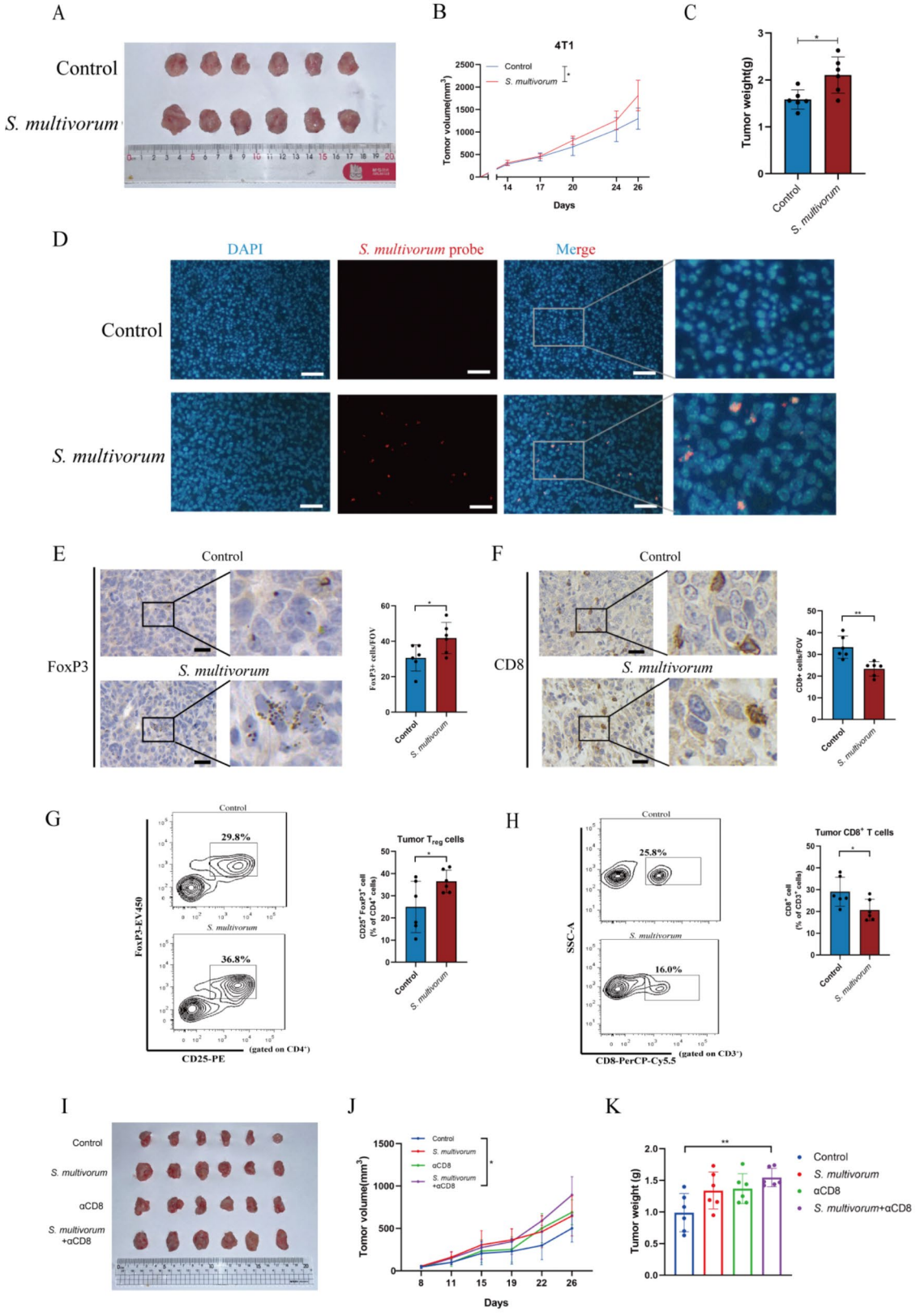

Fig. 2 (See legend on next page.)

(See figure on previous page.)

Fig. 2 Tissue-resident *S. multivorum* accelerated tumor growth in vivo. (**A**) Saline or 2×10^7 CFU of *S. multivorum* was administered intratumorally twice per week to mice bearing 4T1 tumor. (**B**) Tumor growth curve in BALB/c mice ($n=6$). (**C**) Tumor weight in BALB/c mice ($n=6$). (**D**) Fluorescence in situ hybridization staining for DAPI (Blue) and CY3-labeled *S. multivorum* (Red) fluorescent probes for detecting tumor-resident *S. multivorum* in mice, scale bar = 50 μm. (**E**) Immunohistochemical analysis of FoxP3 within mouse tumors, scale bar = 10 μm. (**F**) Immunohistochemical analysis of CD8 within mouse tumors, scale bar = 10 μm. (**G**) Representative flow cytometric contour plot showing tumor-infiltrating Treg cells in 4T1 tumor-bearing mice. (**H**) Representative flow cytometric contour plot showing tumor-infiltrating $CD8^+$ T cells in 4T1 tumor-bearing mice. (**I**) The image represented tumor sizes in the presence or absence of *S. multivorum* alone or CD8 neutralizing antibody or combination. (**J**) Tumor growth curve in BALB/c mice. (**K**) Tumor weight in BALB/c mice. Statistical significance was determined by an unpaired two-tailed Student's t-test for (**C**-**F**) and ANOVA statistical test with a Tukey's post-hoc analysis for (**J**, **K**). Significance levels are denoted as $^*p<0.05$; $^{**}p<0.01$

addition, the 4T1 tumor-bearing mice were administered with either *S. multivorum* or saline directly into the tumor, in conjunction with a CD8 neutralizing antibody for CD8 in vivo depletion once a week. We found that the depletion of $CD8^+$ T cells increased the tumor promotion of *S. multivorum* (Fig. 2I-K). Collectively, these data suggest that intra-tumoral *S. multivorum* may promote tumor growth in 4T1 tumor-bearing mice by modulating Treg cells and $CD8^+$ T cells.

S. Multivorum inhibited the anti-tumor effect of PD-1 antibody

The tumor-promoting effect of *S. multivorum* was further confirmed in mice treated with αPD-1 mAb. In the 4T1 tumor-bearing model, when the tumor size reached 50-100mm^3, the mice were administered with either *S. multivorum* (2×10^7 CFU) or saline directly into the tumor, in conjunction with biweekly intraperitoneal injections of an isotype control IgG or αPD-1 mAb (Fig. 3A). *S. multivorum* was shown to remarkably diminish the therapeutic efficacy of αPD-1 mAb (Fig. 3B-D). To this end, an upregulation of FoxP3 expression (a Treg marker) was detected in the tumor colonized by *S. multivorum*, compared with the control, by immunohistochemical assay (Fig. 3F). Meanwhile, compared with mice that were administered with αPD-1 mAb alone, significantly less $CD8^+$ T cells and lower IFN-γ level were detected in the mice tumors injected with *S. multivorum* and αPD-1 mAb (Fig. 3E, G). In conclusion, intra-tumoral colonization of *S. multivorum* not only accelerated breast cancer growth but also impaired the therapeutic response to αPD-1 mAb.

Propionylcarnitine which was decreased by *S. Multivorum* inhibits tumor growth in vivo

Abundant evidence has shown that tumor-resident bacteria could regulate the host immune system through microbial metabolites [26–28]. To further investigate the effects of *S. multivorum* on the TME, targeted metabolomics analysis was performed in tumor tissues from the 4T1 tumor-bearing mouse model. A total of 451 distinct metabolites were identified. Compared with the control mice, there were twenty differential metabolites found in tumor tissues from the *S. multivorum*-injected mice (Fig. 4A). The abundance of seven metabolites was remarkably increased and that of the other thirteen metabolites was significantly reduced in tumors of mice colonized with *S. multivorum* (Fig. 4B, C). Notably, three carnitine compounds, propionylcarnitine, hexanylcarnitine, and butyrylcarnitine, were decreased in the *S. multivorum* group (Fig. 4D-F). This attenuation suggests a potential regulatory role of *S. multivorum* on carnitine metabolism within the TME.

The biological activities of carnitine metabolites were investigated in breast cancer cells. We found that propionylcarnitine, hexanylcarnitine, and butyrylcarnitine did not promote 4T1 cell proliferation directly in vitro (Fig. 4G). The effects of these carnitine metabolites on BALB/c mice spleen lymphocytes were examined. Interestingly, propionylcarnitine did not affect the viability of lymphocytes (Fig. 4H) but decreased the proportion of Treg cells in vitro (Fig. 4I). However, hexanylcarnitine and butyrylcarnitine did not inhibit the proportion of Treg cells (Fig. 4J, K). To investigate whether *S. multivorum* or/and propionylcarnitine confer to trigger cancer growth, the model of 4T1 mice breast cancer cells-bearing mice was established and divided 4 groups: control (saline, 5 ml/kg, q3d, intratumoral injections), *S. multivorum* alone (2×10^7 CFU, q3d, intratumoral injections), propionylcarnitine alone (150 mg/kg, q3d, intratumoral injections), combination of *S. multivorum* and propionylcarnitine. The results showed the tumor growth was promoted in the presence of *S. multivorum*, while the tumor growth did not significantly change in the group combination of *S. multivorum* and propionylcarnitine compared with the control group (Fig. 4L-O). Overall, these findings indicate that *S. multivorum* may deplete propionylcarnitine within the TME, thereby modulating the Treg cell population in BALB/c mice and inhibiting tumor progression.

S. multivorum induced immunosuppression through enhancements of CCL20 and CXCL8 expression

To investigate the molecular mechanisms by which *S. multivorum* promoted breast cancer growth, we next performed RNA-seq analysis in MDA-MB-231 cells stimulated by *S. multivorum* (Multiplicity of infection = 100) for 6 h. Previous studies have reported that inflammatory signaling pathways are critical for tumor suppression and tumor immune surveillance [29, 30]. Our investigation

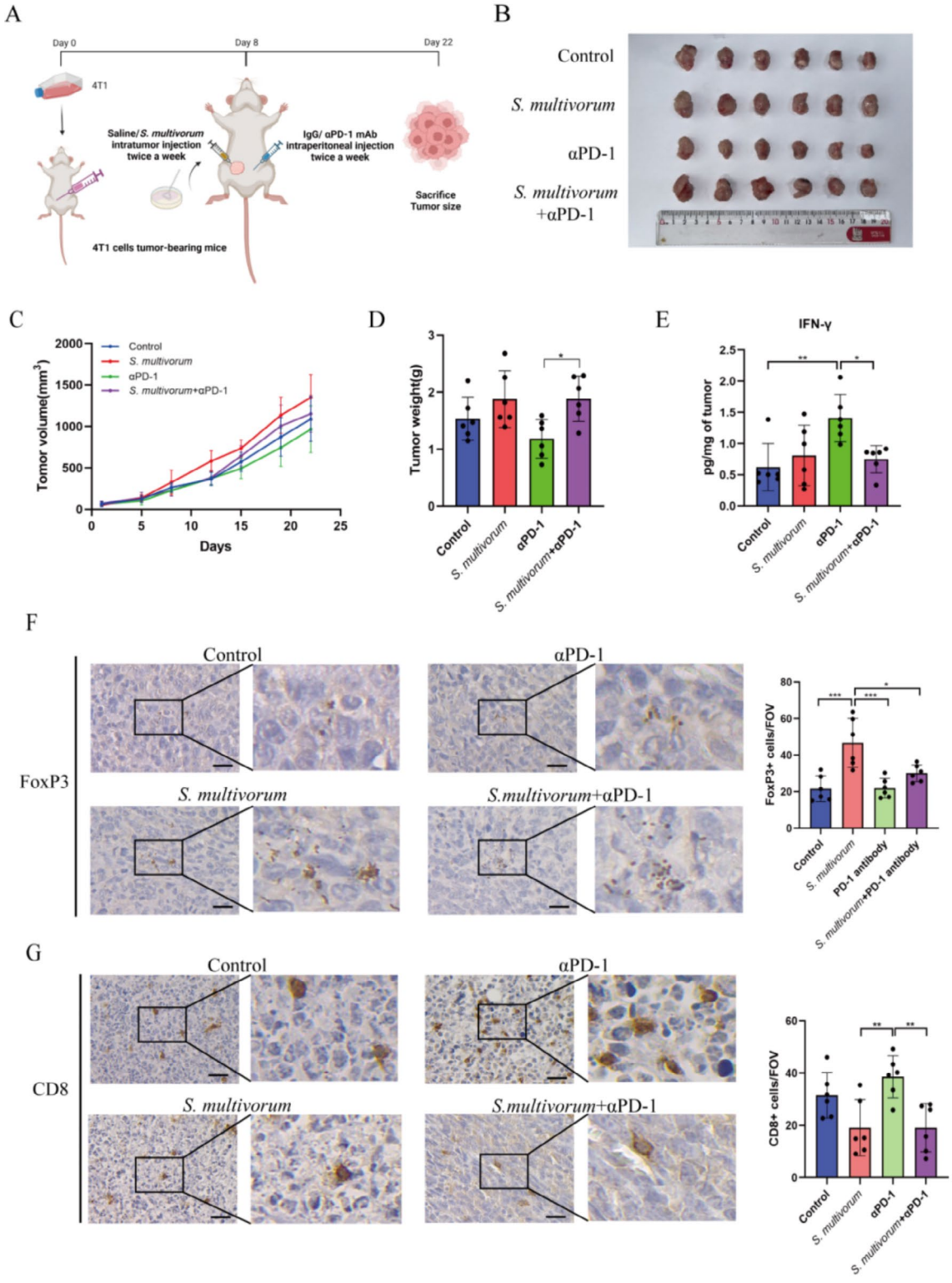

Fig. 3 *S. multivorum* inhibited the anti-tumor effect of PD-1 antibody. (**A**) Schematic diagram showing the experimental design ($n=6$ per group). (**B**) When the tumor volume of mice reached 50-100mm^3, mice were injected intra-tumorally with saline or 2×10^7 CFU *S. multivorum*, in conjunction with intraperitoneal injections of αPD-1 mAb twice a week. (**C**) Tumor growth curve in BALB/c mice. (**D**) Tumor weight in BALB/c mice. (**E**) Levels of IFN-γ in tumor tissues of BALB/c mice. (**F**) Immunohistochemical staining for CD8$^+$ T cell infiltration, scale bar = 10 μm. (**G**) Immunohistochemical staining for FoxP3 expression, scale bar = 10 μm. Statistics for this entire figure were performed using an ANOVA statistical test with a Tukey's post-hoc analysis. Significance levels are denoted as $^*p<0.05$; $^{**}p<0.01$; $^{***}p<0.001$

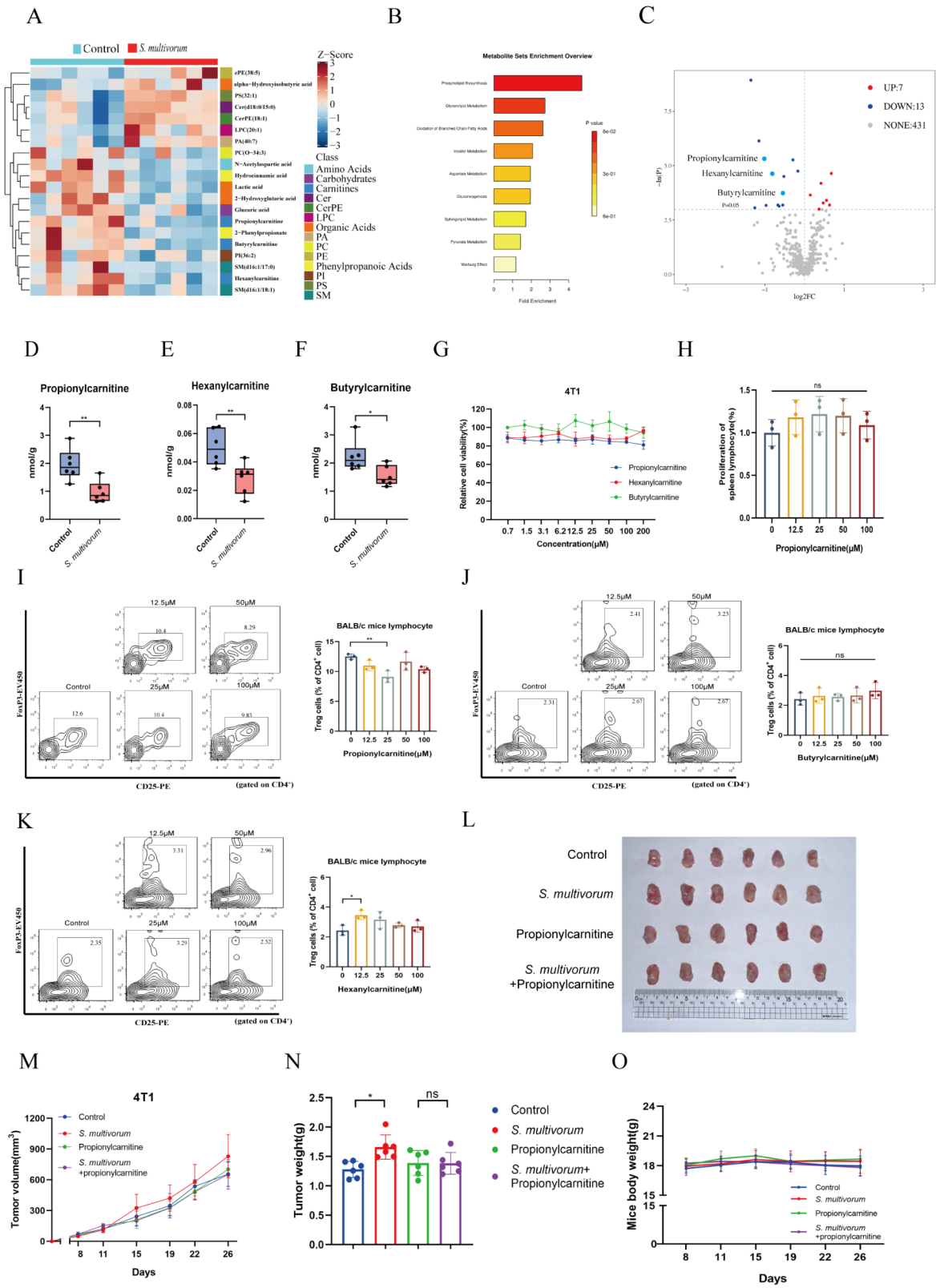

Fig. 4 (See legend on next page.)

(See figure on previous page.)

Fig. 4 Propionylcarnitine which was decreased by *S. multivorum* inhibits tumor growth *in vivo*. (**A**) Heatmap showing potential biomarker levels in mouse tumors. The screening criteria were $p < 0.05$ and $|\log2FC| \geq 0$ for unidimensional analysis, and VIP value > 1 for multidimensional analysis. (**B**) Pathway enrichment analysis of differential metabolites using pathway-associated metabolite sets (SMPDB). (**C**) Volcano plot showing the differential metabolites based on one-dimensional statistical screening. Differential metabolites were considered significant at a threshold of $p < 0.05$ and $|\log2FC| \geq 0$. (**D-F**) Concentration of short-chain acylcarnitine metabolites in mouse tumors. (**G**) The effect of propionylcarnitine on cell viability of MDA-MB-231, BT20, and 4T1 cell lines in vitro. (**H**) The effect of propionylcarnitine on spleen lymphocyte viability in BALB/c mice. (**I**) The number of Treg cells in splenic lymphocytes of BALB/c mice by flow cytometry analysis. (**L**) Images of representative 4T1 subcutaneous tumors after the intra-tumoral injection of the *S. multivorum* in BALB/c mice. PBS served as a negative control. 2×10^7 CFU of *S. multivorum* were injected into subcutaneous tumors as described above. 150 mg/kg propionylcarnitine was injected into the tumor twice a week. After 26 days, the subcutaneous tumors were isolated and shown. (**M**) Tumor growth curve in BALB/c mice. (**N**) Tumor weight in BALB/c mice. (**O**) Body weight of BALB/c mice. Statistical significance was determined by an unpaired two-tailed Student's t-test for (**D-F**) and ANOVA statistical test with a Tukey's post-hoc analysis for (**H**-**K**, **N**). Significance levels are denoted as $^*p < 0.05$; $^{**}p < 0.01$; $^{***}p < 0.001$

revealed a significant up-regulation of genes integral to the IL-17 signaling pathway (Fig. 5A), which was also supported by data from the Gene set enrichment analysis (GSEA) (Fig. 5B). Transcription factors, including Jun, Fos, IL-1β, CXCL8, MMP99, and CCL20, were significantly up-regulated (Fig. 5C). The increased expression of these transcription factors were also validated by qPCR assay in both MDA-MB231 and BT20 cells (Fig. 5D, E). Tumor cell-derived CCL20 has been implicated in recruiting Treg cells to the TME via CCR6 and inhibiting IFN-γ secretion by $CD8^+$ T cells [31–33]. On the other hand, tumor-derived CXCL8 is known to recruit neutrophils to enhance tumor cell proliferation and promotes angiogenesis by activating endothelial cells [13]. It has been reported that Cxcl8 plays an important role in establishing an immunosuppressive TME by decreasing the infiltration of $CD8^+$ T cell and up-regulating PD-L1 expression on macrophages [34]. Interestingly, *S. multivorum* was found to increase the secretion of CCL20 and CXCL8 from MDA-MB-231 and BT20 cells by ELISA assay (Fig. 5F, G). Moreover, in the 4T1 tumor-bearing mouse model, CCL20 levels in the tumor (Fig. 5H) and abundance of Treg cells (Fig. 5I) in peripheral blood were found to be significantly higher in mice injected with *S. multivorum* than the control. We further investigated the metabolite propionylcarnitine, which was significantly reduced after *S.multivorum* colonization within the TME, our study revealed propionylcarnitine inhibited chemokines CCL20 and CXCL8 expressions (Fig. 5J, K). Overall, our data suggested that *S. multivorum* recruited Treg cells to the TME by activating the IL-17 signaling pathway and stimulating the secretion of the chemokine CCL20 from the tumor.

In summary, we revealed that intra-tumoral *S. multivorum* promotes tumorigenesis and diminishes the therapeutic efficacy of αPD-1 mAb by decreasing the ratio of $CD8^+$ T cells/Treg cells in the TME (Fig. 6). Mechanistically, *S. multivorum* promotes the secretion of chemokine CCL20 from tumor cells. The secreted CCL20 recruits Treg cells and reduces $CD8^+$ T cell infiltration into the tumors. The findings deepen our insight about the influence of intratumor-resident microbes on the TME, which interact with the host immune system to regulate cancer progression.

Discussion

There is increasing evidence showing the presence of a unique microbial colonization in breast tissue, which was previously thought to be sterile. Moreover, the microbial profiles in the tumors from breast cancer patients were found to be distinct from the normal mammary tissue of healthy individuals [35]. Within this intricate nexus, tumor-resident microbiota has been reported to remodel the TME or stimulate the recruitment and activation of immune cells, thereby exerting a crucial role in cancer development, treatment, and prognosis [36, 37]. *S. multivorum* is ubiquitous in nature and the biological significance of its residence inside tumors is poorly studied.

In this study, we found that *S. multivorum* showed a high relative abundance in cancerous tissues of breast cancer patients. Intriguingly, increasing relative abundance of *Sphingobacterium* has been reported in patients with triple-negative breast cancer, colon adenocarcinomas, and bladder cancer [16–18], indicating a potential link between *S. multivorum* and an increased risk of tumorigenesis. Moreover, intratumor colonization by *S. multivorum* was shown to stimulate tumor development and increased the ratio of tumor-infiltrating $CD8^+$ T cells/Treg cells. Our findings suggest that tumor-resident microbiota may have distinct functions in the TME and they could interact with the host immune system to regulate antitumor response. It follows that some tumor-resident microbiota may serve as prospective targets for cancer immunotherapy.

Data from the metabolomic profiling studies revealed a significant reduction of propionylcarnitine concentration in tumors of mice colonized with *S. multivorum*. As a prevalent form of short-chain acylcarnitine, propionylcarnitine constitutes a substantial proportion of acylcarnitine content, accounting for over half of these compounds in human tissue matrices and body fluids [38]. Originating from the metabolism of specific amino acids, such as lysine and valine, into propionyl coenzyme A (PCoA), propionylcarnitine is synthesized via the

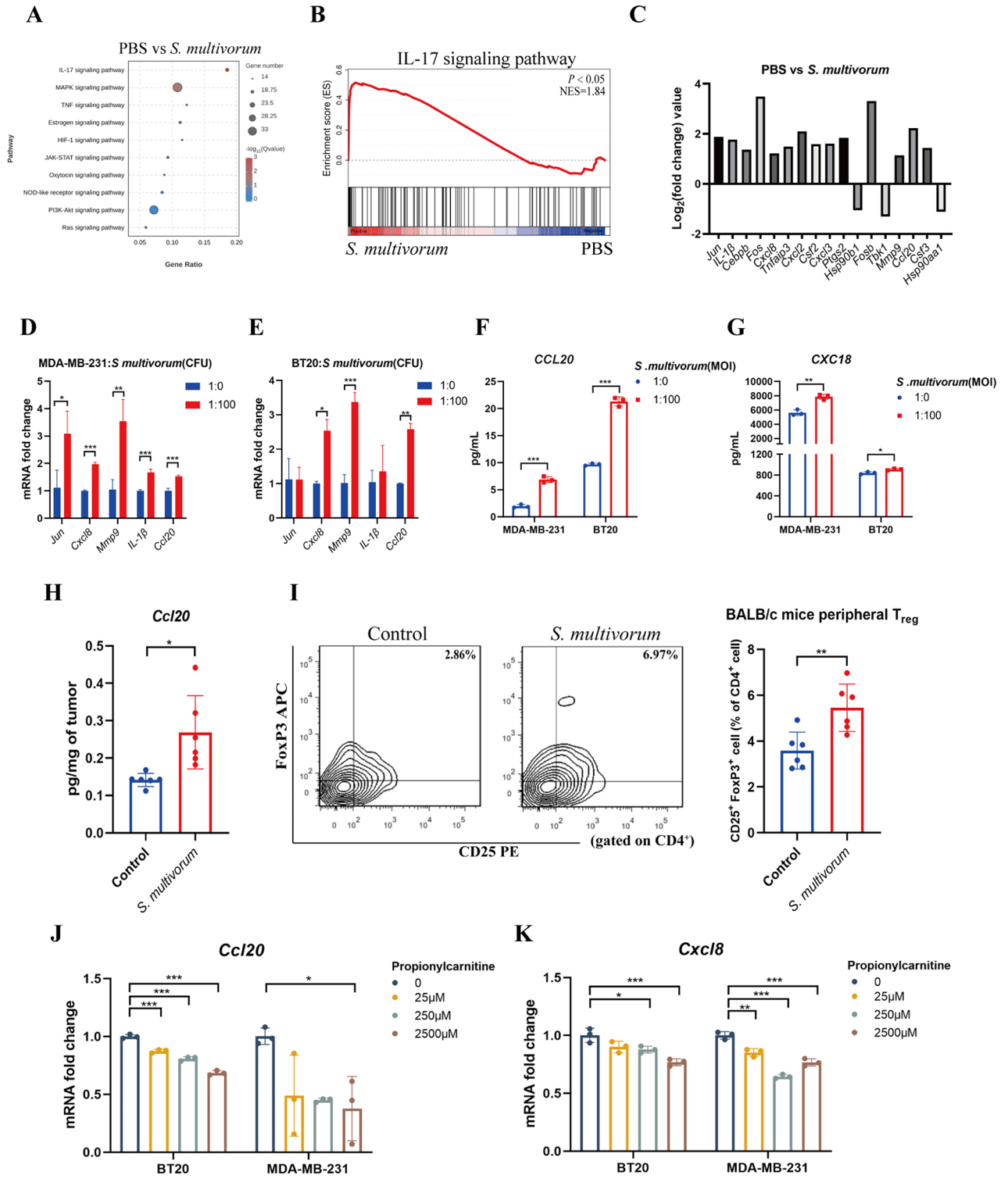

Fig. 5 (See legend on next page.)

enzymatic action of carnitine acetyltransferase (CrAT) [39]. To this end, the reduction of propionylcarnitine in hepatocellular carcinoma tissues has been recognized as a biomarker for identifying hepatitis and hepatocellular carcinoma [40]. Reduced PCoA has also been reported to contribute to metabolic remodeling and promote hepatocellular carcinoma [41]. Our results indicate that the diminished levels of propionylcarnitine within the TME,

(See figure on previous page.)

Fig. 5 *S. multivorum* induced immunosuppression through enhancements of CCL20 and CXCL8 expression. (**A**) Total RNA samples were harvested from MDA-MD-231 cells after stimulation by *S. multivorum* (multiplicity of infection = 100) on 6 h, and subjected for RNA sequencing analysis. KEGG pathway enrichment analysis revealed that the IL-17 signaling pathway was significantly activated in the *S. multivorum* group. (**B**) Gene set enrichment analysis (GSEA) of transcriptomic data showing activation of the IL-17 signaling pathway; $p < 0.05$, NES = 1.84. (**C**) The fold change of differentially expressed genes within IL-17 signaling pathway. (**D**) Relative mRNA expression of IL-17 signaling pathway-related genes in MDA-MB-231 cells and *S. multivorum* co-culture systems by qPCR analysis. (**E**) Relative mRNA expression of IL-17 signaling pathway-related genes in BT20 cells and *S. multivorum* co-culture systems by qPCR analysis. (**F**, **G**) Chemokine CCL20 and CXCL8 levels in MDA-MB-23, and BT20 and *S. multivorum* co-culture systems by ELISA assay. (**H**) CCL20 level in the TME of 4T1 tumor-bearing mice by ELISA assay. (**I**) The proportion of Treg cells in peripheral blood of 4T1 tumor-bearing mice by flow cytometric analysis. (**J**, **K**) The relative mRNA expression levels of *CXCL8* and *CCL20* in BT20 and MDA-MB-231 cells treated with different concentrations of propionylcarnitine were measured by qPCR. Statistical significance was determined by an unpaired two-tailed Student's *t*-test for (**B**-**I**) and ANOVA statistical test with a Tukey's post-hoc analysis for (**J**, **K**). Significance levels are denoted as $*p < 0.05$; $**p < 0.01$; $***p < 0.001$

specifically in mice injected with *S. multivorum*, could play a role in cancer progression, given its capacity to reduce Treg cell viability in vitro.

Intratumoral microorganisms often influence the levels of chemokines within the TME. Elucidating the influence of intratumoral microorganisms on chemokines in tumors is beneficial to our further understanding of tumor progression. We also showed that Treg cells were remarkably increased in mice injected with *S. multivorum*. This finding lends weight to the hypothesis that *S. multivorum* might recruit Treg cells or induce the differentiation of naïve $CD4^+$ T cells into Treg cells within the tumor. Our qPCR and ELISA assay results indicate that *S. multivorum* induced the secretion of chemokines such as CCL20 and CXCL8 from tumor cells. CCL20, also known as macrophage inflammatory protein 3α (MIP-3α), is a member of the CC chemokine family [42, 43]. The production of CCL20 is attributed to tumor cells and tumor-associated macrophages, exerting the principal role in recruiting Treg and Th17 cells into the TME [44, 45]. Meanwhile, the cognate chemokine receptor for CCL20 is identified as CCR6 [46]. High infiltration of $CCR6^+$ Treg within tumors can promote immune tolerance and breast cancer progression by inhibiting the activity of

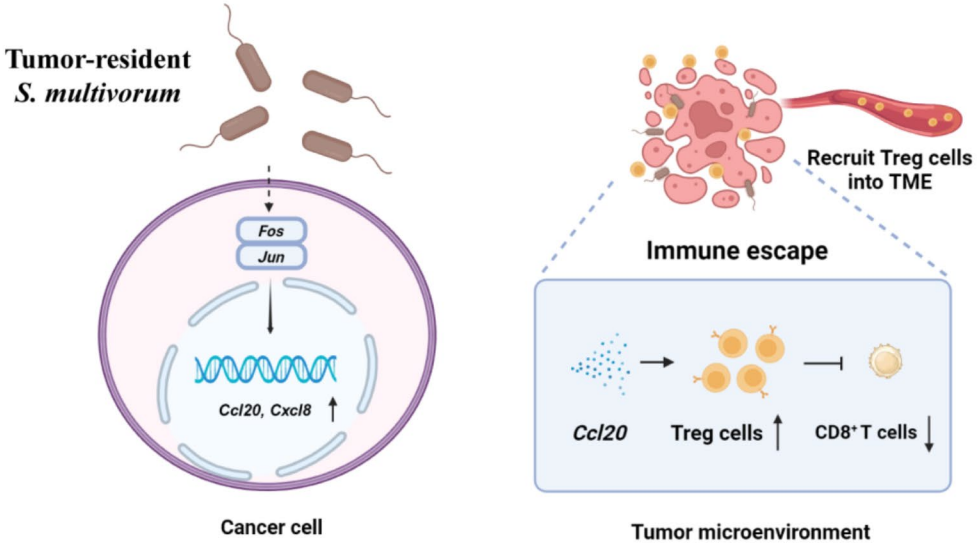

Fig. 6 Potential biological mechanisms of *S. multivorum* for breast cancer growth. *S. multivorum* promotes the secretion of chemokines CCL20 and CXCL8 from tumor cells. Tumor-derived CCL20 recruits Treg cells into the TME and reduces $CD8^+$ T cell infiltration, thereby leading to an immunosuppressive TME

IFN-γ in $CD8^+$ T cells [33]. Some microorganisms, such as *F. nucleatum*, can promote tumor invasion by recruiting Treg cells with the chemokine CCL20 [47]. On the other hand, CXCL8 plays different roles in the TME, such as suppressing the immune response to promote tumor angiogenesis and metastasis [48–50].

The present findings have significant implications for the clinical management of breast cancer patients undergoing immunotherapy. The abundance of *S.multivorum* and the concentration of propionylcarnitine are closely associated with the efficacy of immunotherapy. Consequently, *S. multivorum* and propionylcarnitine may serve as potential biomarkers to predict the therapeutic efficacy of immunotherapy.

Limitations of the study

Due to the complexity of the crosstalk between tumor-resident bacteria and the host immune system, *S.multivorum* is unlikely to be the sole microbiota that can diminish the immunotherapy efficacy in breast cancer. More specifically, in the study of IFN-γ level within the tumor microenvironment, ELISA assay only provided the total concentration of IFN-γ in the tumor tissue homogenate and cannot distinguish which cell subsets are secreting IFN-γ. Although our study demonstrated that *S.multivorum* promotes breast tumor growth by influencing the tumor microenvironment, it remains possible that *S. multivorum* may also contribute to tumor metastasis. More in-depth research and precise analysis are still required to address this aspect fully.

Abbreviations

BC	Breast cancer
TME	Tumor microenvironment
Treg	Regulatory T cell
Sphingobacterium multivorum	S. multivorum
TILs	Tumor-infiltrating lymphocytes
iTreg	Induced regulatory T cell
PCoA	Principal Coordinate Analysis
nTreg	Natural regulatory T cell
CFU	Colony forming units
SMPDB	Pathway-associated metabolite sets
GSEA	Gene set enrichment analysis
PCoA	Propionyl coenzyme A
CrAT	Carnitine acetyltransferase
KEGG	Kyoto Encyclopedia of Genes and Genomes
MIP-3α	Macrophage inflammatory protein 3α

Supplementary Information

The online version contains supplementary material available at https://doi.org/10.1186/s12943-024-02202-9.

Supplementary Material 1

Supplementary Material 2

Acknowledgements

We especially thank Gene Denovo Biotechnology(Guangzhou, China) for their assistance with 16S rDNA sequence techniques in this study. We also thank Metabo-Profile Co., Ltd (Shanghai, China) for their assistance with targeted metabolomicsexperiment in this study. We are grateful to BioRender (https://app.biorender.com/) for their invaluable assistance in our characterisation of the molecular mechanism.

Author contributions

Z. M. performed most of the animal experiments and molecular biology experiments, and drafted the manuscript. C.Y. collected the clinical samples. C. X. designed and supervised the project. L. F., J. S. contributed to experiments guidance. L. F., K. T. critically revised this manuscript. All author reviewed and consented to the manuscript in its finalized form.

Funding

Foshan Antitumor Innovative Drug Research and Engineering Technology Center (No. FS0AA-KJ819-4901-0082).

Data availability

No datasets were generated or analysed during the current study.

Declarations

Ethics approval and consent to participate

The investigation complied with pertinent ethical standards governing human participant research. The collection and use of patient-derived tumor specimens for research was approved by Ethics Committee of Yuebei People's Hospital (Reference KY-2022-057).

Consent for publication

Not applicable.

Competing interests

The authors declare no competing interests.

Author details

[1]Foshan Maternity and Child Healthcare Hospital; School of Pharmaceutical Sciences, Southern Medical University, Guangzhou 515150, China
[2]State Key Laboratory of Oncology in South China, Collaborative Innovation Center for Cancer Medicine, Guangdong Esophageal Cancer Institute, Sun Yat-sen University Cancer Center, Guangzhou 510060, China
[3]School of Pharmacy, The Chinese University of Hong Kong, Hong Kong 999077, China
[4]Department of Breast, Thyroid and Head-Neck Surgery, Yuebei People's Hospital of Shantou University, Shaoguan, China

Received: 9 August 2024 / Accepted: 18 December 2024
Published online: 08 January 2025

References

1. Fahad Ullah M. Breast Cancer: current perspectives on the Disease Status. Adv Exp Med Biol. 2019;1152:51–64.
2. Fu A, Yao B, Dong T, Chen Y, Yao J, Liu Y, Li H, Bai H, Liu X, Zhang Y, et al. Tumor-resident intracellular microbiota promotes metastatic colonization in breast cancer. Cell. 2022;185:1356–e137226.
3. Xie Y, Xie F, Zhou X, Zhang L, Yang B, Huang J, Wang F, Yan H, Zeng L, Zhang L, et al. Microbiota in tumors: from understanding to application. Adv Sci (Weinh). 2022;9:e2200470.
4. Greathouse KL, Stone JK, Harris CC. Cancer-type-specific Bacteria: freeloaders or partners. Cancer Cell. 2020;38:158–60.
5. Pushalkar S, Hundeyin M, Daley D, Zambirinis CP, Kurz E, Mishra A, Mohan N, Aykut B, Usyk M, Torres LE, et al. The pancreatic Cancer Microbiome promotes oncogenesis by induction of Innate and Adaptive Immune suppression. Cancer Discov. 2018;8:403–16.
6. Parhi L, Alon-Maimon T, Sol A, Nejman D, Shhadeh A, Fainsod-Levi T, Yajuk O, Isaacson B, Abed J, Maalouf N, et al. Breast cancer colonization by Fusobacterium nucleatum accelerates tumor growth and metastatic progression. Nat Commun. 2020;11:3259.
7. Geller LT, Barzily-Rokni M, Danino T, Jonas OH, Shental N, Nejman D, Gavert N, Zwang Y, Cooper ZA, Shee K, et al. Potential role of intratumor bacteria

in mediating tumor resistance to the chemotherapeutic drug gemcitabine. Science. 2017;357:1156–60.
8. Jiang SS, Xie YL, Xiao XY, Kang ZR, Lin XL, Zhang L, Li CS, Qian Y, Xu PP, Leng XX, et al. Fusobacterium nucleatum-derived succinic acid induces tumor resistance to immunotherapy in colorectal cancer. Cell Host Microbe. 2023;31:781–e7979.
9. Wang H, Rong X, Zhao G, Zhou Y, Xiao Y, Ma D, Jin X, Wu Y, Yan Y, Yang H, et al. The microbial metabolite trimethylamine N-oxide promotes antitumor immunity in triple-negative breast cancer. Cell Metab. 2022;34:581–e5948.
10. Kang JH, Zappasodi R. Modulating Treg stability to improve cancer immunotherapy. Trends Cancer. 2023;9:911–27.
11. Komatsu N, Okamoto K, Sawa S, Nakashima T, Oh-hora M, Kodama T, Tanaka S, Bluestone JA, Takayanagi H. Pathogenic conversion of Foxp3 + T cells into TH17 cells in autoimmune arthritis. Nat Med. 2014;20:62–8.
12. Xu W, Wu Y, Wang L, Bai Y, Du Y, Li Y, Cao N, Zhao Y, Zhang Y, Liu H. Autoantibody against β(1)-adrenoceptor promotes the differentiation of natural regulatory T cells from activated CD4(+) T cells by up-regulating AMPK-mediated fatty acid oxidation. Cell Death Dis. 2019;10:158.
13. Li C, Jiang P, Wei S, Xu X, Wang J. Regulatory T cells in tumor microenvironment: new mechanisms, potential therapeutic strategies and future prospects. Mol Cancer. 2020;19:116.
14. Budhu S, Schaer DA, Li Y, Toledo-Crow R, Panageas K, Yang X, Zhong H, Houghton AN, Silverstein SC, Merghoub T et al. Blockade of surface-bound TGF-β on regulatory T cells abrogates suppression of effector T cell function in the tumor microenvironment. 2017;10(494):eaak9702.
15. Li Y, Guo X, Qiu Y, Fang C, Liu D, Liu Q, Dai X, Zhang L. Characterization of a novel multidrug-resistant genomic island in Sphingobacterium spp. strains recovered from pleural fluid of lung cancer patients. J Glob Antimicrob Resist. 2023;32:18–20.
16. Wu P, Zhang G, Zhao J, Chen J, Chen Y, Huang W, Zhong J, Zeng J. Profiling the urinary microbiota in male patients with bladder Cancer in China. Front Cell Infect Microbiol. 2018;8:167.
17. Hua H, Sun Y, He X, Chen Y, Teng L, Lu C. Intestinal microbiota in colorectal adenoma-carcinoma sequence. Front Med (Lausanne). 2022;9:888340.
18. Banerjee S, Wei Z, Tan F, Peck KN, Shih N, Feldman M, Rebbeck TR, Alwine JC, Robertson ES. Distinct microbiological signatures associated with triple negative breast cancer. Sci Rep. 2015;5:15162.
19. Chai X, Wang J, Li H, Gao C, Li S, Wei C, Huang J, Tian Y, Yuan J, Lu J, et al. Intratumor microbiome features reveal antitumor potentials of intrahepatic cholangiocarcinoma. Gut Microbes. 2023;15:2156255.
20. Guo M, Wu F, Hao G, Qi Q, Li R, Li N, Wei L, Chai T. Bacillus subtilis improves immunity and Disease Resistance in rabbits. Front Immunol. 2017;8:354.
21. Chen S, Zhou Y, Chen Y, Gu J. Fastp: an ultra-fast all-in-one FASTQ preprocessor. Bioinformatics. 2018;34:i884–90.
22. Edgar RC. UPARSE: highly accurate OTU sequences from microbial amplicon reads. Nat Methods. 2013;10(10):996–8.
23. Segata N, Izard J, Waldron L, Gevers D, Miropolsky L, Garrett WS, Huttenhower C. Metagenomic biomarker discovery and explanation. Genome Biol. 2011;12:R60.
24. Xie G, Wang L, Chen T, Zhou K, Zhang Z, Li J, Sun B, Guo Y, Wang X, Wang Y, et al. A metabolite array technology for Precision Medicine. Anal Chem. 2021;93:5709–17.
25. Wiklund S, Johansson E, Sjöström L, Mellerowicz EJ, Edlund U, Shockcor JP, Gottfries J, Moritz T, Trygg J. Visualization of GC/TOF-MS-based metabolomics data for identification of biochemically interesting compounds using OPLS class models. Anal Chem. 2008;80:115–22.
26. Bell HN, Rebernick RJ, Goyert J, Singhal R, Kuljanin M, Kerk SA, Huang W, Das NK, Andren A, Solanki S, et al. Reuterin in the healthy gut microbiome suppresses colorectal cancer growth through altering redox balance. Cancer Cell. 2022;40:185–e2006.
27. Fong W, Li Q, Ji F, Liang W, Lau H, Kang X, Liu W, To KK, Zuo Z, Li X et al. Lactobacillus gallinarum-derived metabolites boost anti-PD1 efficacy in colorectal cancer by inhibiting regulatory T cells through modulating IDO1/Kyn/AHR axis. Gut. 2023.
28. Hezaveh K, Shinde RS, Klötgen A, Halaby MJ, Lamorte S, Ciudad MT, Quevedo R, Neufeld L, Liu ZQ, Jin R, et al. Tryptophan-derived microbial metabolites activate the aryl hydrocarbon receptor in tumor-associated macrophages to suppress anti-tumor immunity. Immunity. 2022;55:324–e3408.
29. Geis AL, Fan H, Wu X, Wu S, Huso DL, Wolfe JL, Sears CL, Pardoll DM, Housseau F. Regulatory T-cell response to Enterotoxigenic Bacteroides fragilis colonization triggers IL17-Dependent Colon carcinogenesis. Cancer Discov. 2015;5:1098–109.
30. Akeus P, Szeponik L, Ahlmanner F, Sundström P, Alsén S, Gustavsson B, Sparwasser T, Raghavan S, Quiding-Järbrink M. Regulatory T cells control endothelial chemokine production and migration of T cells into intestinal tumors of APC(min/+) mice. Cancer Immunol Immunother. 2018;67:1067–77.
31. Wang D, Yang L, Yu W, Wu Q, Lian J, Li F, Liu S, Li A, He Z, Liu J, et al. Colorectal cancer cell-derived CCL20 recruits regulatory T cells to promote chemoresistance via FOXO1/CEBPB/NF-κB signaling. J Immunother Cancer. 2019;7:215.
32. Kwantwi LB, Wang S, Sheng Y, Wu Q. Multifaceted roles of CCL20 (C-C motif chemokine ligand 20): mechanisms and communication networks in breast cancer progression. Bioengineered. 2021;12:6923–34.
33. Xu L, Xu W, Qiu S, Xiong S. Enrichment of CCR6 + Foxp3 + regulatory T cells in the tumor mass correlates with impaired CD8 + T cell function and poor prognosis of breast cancer. Clin Immunol. 2010;135:466–75.
34. Lin C, He H, Liu H, Li R, Chen Y, Qi Y, Jiang Q, Chen L, Zhang P, Zhang H, et al. Tumour-associated macrophages-derived CXCL8 determines immune evasion through autonomous PD-L1 expression in gastric cancer. Gut. 2019;68:1764–73.
35. Urbaniak C, Gloor GB, Brackstone M, Scott L, Tangney M, Reid G. The microbiota of Breast Tissue and its association with breast Cancer. Appl Environ Microbiol. 2016;82:5039–48.
36. Yang L, Li A, Wang Y, Zhang Y. Intratumoral microbiota: roles in cancer initiation, development and therapeutic efficacy. Signal Transduct Target Ther. 2023;8:35.
37. Ji H, Jiang Z, Wei C, Ma Y, Zhao J, Wang F, Zhao B, Wang D, Tang D. Intratumoural microbiota: from theory to clinical application. Cell Commun Signal. 2023;21:164.
38. Makarova E, Makrecka-Kuka M, Vilks K, Volska K, Sevostjanovs E, Grinberga S, Zarkova-Malkova O, Dambrova M, Liepinsh E. Decreases in circulating concentrations of long-chain acylcarnitines and free fatty acids during the glucose tolerance test represent tissue-specific insulin sensitivity. Front Endocrinol (Lausanne). 2019;10:870.
39. Dambrova M, Makrecka-Kuka M, Kuka J, Vilskersts R, Nordberg D, Attwood MM, Smesny S, Sen ZD, Guo AC, Oler E, et al. Acylcarnitines: nomenclature, biomarkers, therapeutic potential, drug targets, and clinical trials. Pharmacol Rev. 2022;74:506–51.
40. Ferrarini A, Di Poto C, He S, Tu C, Varghese RS, Kara Balla A, Jayatilake M, Li Z, Ghaffari K, Fan Z, et al. Metabolomic Analysis of Liver Tissues for Characterization of Hepatocellular Carcinoma. J Proteome Res. 2019;18:3067–76.
41. Sun J, Ding J, Shen Q, Wang X, Wang M, Huang Y, Zhang X, Zhu H, Zhang F, Wu D, et al. Decreased propionyl-CoA metabolism facilitates metabolic reprogramming and promotes hepatocellular carcinoma. J Hepatol. 2023;78:627–42.
42. Zlotnik A, Yoshie O. Chemokines: a new classification system and their role in immunity. Immunity. 2000;12:121–7.
43. Yang C, Deng X, Tang Y, Tang H, Xia C. Natural products reverse cisplatin resistance in the hypoxic tumor microenvironment. Cancer Lett. 2024;598:217116.
44. Korbecki J, Grochans S, Gutowska I, Barczak K, Baranowska-Bosiacka I. CC chemokines in a Tumor: a review of Pro-cancer and Anti-cancer properties of receptors CCR5, CCR6, CCR7, CCR8, CCR9, and CCR10 ligands. Int J Mol Sci. 2020;21.
45. Cao S, Liu M, Sehrawat TS, Shah VH. Regulation and functional roles of chemokines in liver diseases. Nat Rev Gastroenterol Hepatol. 2021;18:630–47.
46. Schutyser E, Struyf S, Van Damme J. The CC chemokine CCL20 and its receptor CCR6. Cytokine Growth Factor Rev. 2003;14:409–26.
47. Yamamura K, Baba Y, Nakagawa S, Mima K, Miyake K, Nakamura K, Sawayama H, Kinoshita K, Ishimoto T, Iwatsuki M, et al. Human Microbiome Fusobacterium Nucleatum in Esophageal Cancer tissue is Associated with Prognosis. Clin Cancer Res. 2016;22:5574–81.
48. Huang W, Chen Z, Zhang L, Tian D, Wang D, Fan D, Wu K, Xia L. Interleukin-8 induces expression of FOXC1 to promote transactivation of CXCR1 and CCL2 in Hepatocellular Carcinoma Cell lines and formation of metastases in mice. Gastroenterology. 2015;149:1053–e106714.
49. Maxwell PJ, Coulter J, Walker SM, McKechnie M, Neisen J, McCabe N, Kennedy RD, Salto-Tellez M, Albanese C, Waugh DJ. Potentiation of inflammatory CXCL8 signalling sustains cell survival in PTEN-deficient prostate carcinoma. Eur Urol. 2013;64:177–88.

50. Han ZJ, Li YB, Yang LX, Cheng HJ, Liu X, Chen H. Roles of the CXCL8-CXCR1/2 Axis in the Tumor Microenvironment and Immunotherapy. Molecules. 2021;27.

Publisher's note